

# Axial Ratio Tuned Circularly Polarized Slot-Loaded Antenna for S-Band and C-Band Applications

Ramya Radhakrishnan\* and Shilpi Gupta

**Abstract**—This paper introduces a dual-band circularly polarized antenna modeled on an FR4 substrate with an optimized dimension of  $48\text{ mm} \times 29.5\text{ mm} \times 1.6\text{ mm}$ . A maximum usable circularly polarized bandwidth of 90% is obtained in the lower band (3.08 GHz to 3.75 GHz). A square slot etched in the ground plane loaded with asymmetric plus-shaped slits and tabs aids the impedance bandwidth enhancement. The dual-band operation is accomplished by facilitating parasitic square patches in the slot. The simulated impedance bandwidth of the proposed antenna is 740 MHz (3.07 GHz to 3.81 GHz) for the lower band and 1.57 GHz (4.64 GHz to 6.21 GHz) in the upper band. The impedance and axial ratio bandwidth percentages for lower and upper-frequency bands are 21.5%, 19.6%, and 29.4%, 10.54%, centered at 3.5 GHz and 5.5 GHz, respectively. The simulated and measured results are in reasonably good agreement.

## 1. INTRODUCTION

The employment of circularly polarized antennas in wireless communications has seen exponential growth in the last decade. Advantages like reliable performance, eased orientation flexibility, and minimized multipath fading effects make it robust in diverse environments. The type of input excitation categorizes circularly polarized (C.P.) antennas into two types, dual feed and single feed [1] patch antennas. External feeding networks like hybrid branch-line coupler, Gysel coupler, Wilkinson power divider, etc. provide large axial ratio bandwidth and make the design bulkier. A single feed network design makes use of the structural geometry to give the phase shift of  $90^\circ$ , and a few such techniques include perturbation of the patch [2], cutting a slot or slit [3], truncation of edges [4, 5], stub matching, etc.

Circularly polarized microstrip slot antennas are extensively utilized in Radio-Frequency Identification (RFID) tags and readers, Global Positioning System (GPS), Satellite communication, Global Navigation Satellite System (GNSS), and Wireless Local Area Network (LAN) applications. Slot antennas have their flairs in improving the bandwidth, sustaining a reduced interface through surface waves, providing better isolation, and having lesser radiation from the feed network. A wide square slot produces wide impedance bandwidth because they have two resonating modes merging, leading to broader bandwidth. Nevertheless, the last decade has witnessed many novel designs that produce circular polarization with fractal slot antenna [6], metamaterial inspired slot antenna [7], Co-planar Waveguide (CPW)-fed slot antenna [8], reconfigurable diode controlled slot for switching applications [9], and loading the main slot with multiple tabs or arms [10].

A printed monopole antenna [11] makes use of a T-shape slot in the ground and a pair of rectangular slits in the patch that provides ultra-wide bandwidth and matches with a 50-ohm feed line. However, the monopole configuration along with the slot is an added advantage that yields ultra-wide bandwidth. The

---

*Received 9 May 2021, Accepted 1 July 2021, Scheduled 3 July 2021*

\* Corresponding author: Ramya Radhakrishnan (ramyarakhi9@gmail.com).

The authors are with the Electronics Department, Sardar Vallabhbhai National Institute of Technology, Ichchhanath Circle, Piplod, Surat, Gujarat 395007, India.

antenna proposed in [12] comprises a rectangular slot and a microstrip line with protruded horizontal stubs in the ground. Here it is witnessed that a broader bandwidth is obtained by positioning the extended stub beneath the feedline. The single-feed triple-frequency circularly polarized slot antenna in [13] exhibits two acentric annular rings with an L-shaped feedline. A simple triple-sense wideband C.P. stair-shaped slot antenna consisting of an L-shaped microstrip line radiator is presented in the paper [14]. Two asymmetrically aligned rectangular strips embedding a frame-like structure and the rectangular opening at one end help broaden the axial ratio bandwidth. The antenna communicated in [15] is a simple single-layer antenna with an L-shaped slot and a diagonal strip loaded to produce circular polarization. The parasitic slant strip aligned with the help in procuring the wider bandwidth.

A CPW feed type circularly polarized slot antenna [16] depicted an axial ratio bandwidth (ARBW) of 36.01% with the help of a T-shaped extended metal strip aligned with the slot center. Similarly, a monopole antenna in [17] shows a circularly polarized dual-band antenna that excites the orthogonal modes with the help of a protuberant L-shaped strip and its inverted-shape strip at the radiating edges. These strips also contribute to bandwidth enhancement. One way to achieve broader bandwidth is embedding a fractal Spidron slot as depicted in [18] as it achieved an axial ratio bandwidth of 28.81%.

The proposed work attempts to attain a broader impedance and axial ratio bandwidth, making the antenna compact. A wide square slot embedded with tab-shaped slits at the corners is etched in the ground plane with parasitic square patches to provide circular polarization. Subsequently, the opposite two quadrants were provided with a slanted strip and an H-shaped structure to improve the bandwidth. The primary focus of this work was to achieve a maximum usable C.P. bandwidth with a single-layer slot configuration. The technical contents of the paper are categorized into five parts. The first part imparts a brief introduction to the intended work. The second part communicates the antenna design, geometry, and mathematical modeling. Subsequently, parts three and four touch upon the result discussion and validation.

## 2. ANTENNA DESIGN & GEOMETRY

Figure 1 represents the proposed antenna geometry fabricated on an FR4 substrate with a height of 1.6 mm and a dielectric constant of 4.4. The overall dimensions of the design prototype represent a length ( $L$ )  $\times$  width ( $W$ )  $\times$  thickness ( $h$ ) of 48 mm  $\times$  29.5 mm  $\times$  1.6 mm. The top layer is a microstrip

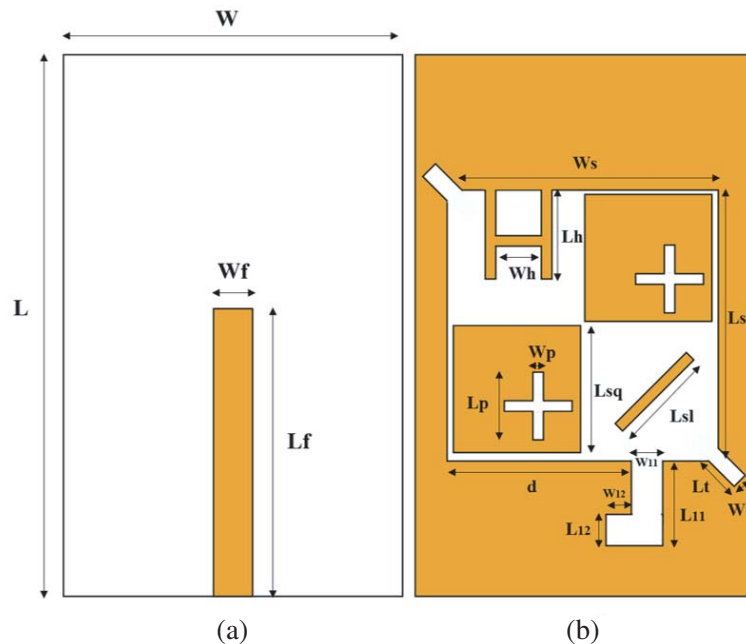


**Figure 1.** Geometry of the antenna proposed. (a) Microstrip feedline. (b) Top view of ground plane.

feed line with a width ( $W_f$ )  $\times$  length ( $L_f$ ) of 3.32 mm  $\times$  26 mm. A square-shaped slot with width ( $W_s$ )  $\times$  length ( $L_s$ ) of 23 mm  $\times$  23 mm extended with tabs ( $W_t$ )  $\times$  length ( $L_t$ ) added at 45° is cut in the bottom layer. The wide slot removed from the ground is divided into four quadrants, where the first and third quadrants are loaded with two square patches with plus-shaped slots etched on them. The second and fourth quadrants have an H-shape stub with ( $W_h$ )  $\times$  length ( $L_h$ ) and a diagonal strip ( $L_{s1}$ ) loaded on them. An L-shaped slot is etched in the ground plane; around  $\lambda/8$  of the resonating frequency provides the exact amount of phase shift required to inline the impedance bandwidth to the axial ratio bandwidth. It plays an essential role in improving polarization purity. The parasitic square patches loaded on the comprehensive slot help enhance the bandwidth of the antenna. The L-shaped slot beneath the microstrip line helps improve the polarization purity and tune the impedance bandwidth with the axial ratio bandwidth.

## 2.1. Modeling of the Proposed Antenna

The proposed and fabricated antenna parameters depicted in Table 1 and Fig. 2, respectively, are approximated and optimized using the equations provided below.

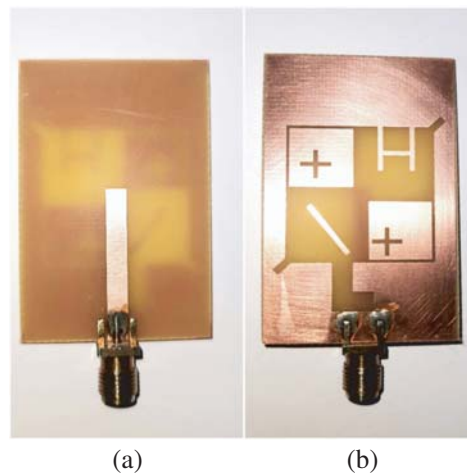


**Figure 2.** Fabricated model of the proposed antenna. (a) Top view of the proposed antenna. (b) Bottom view of the proposed antenna.

**Table 1.** Optimized dimensions of the proposed antenna.

Parameter	Value (mm)	Parameter	Value (mm)
L	48	$L_t$	2.75
W	29.5	$W_t$	1.25
$L_f$	26	$L_h$	7.5
$W_f$	3.25	$W_h$	4.25
$L_s$	23	$L_p$	4.8
$W_s$	23	$W_p$	0.75
$L_{sq}$	9.75	$L_{s1}$	10
$L_{11}$	8	$L_{12}$	3.25
$W_{11}$	3.25	$W_{12}$	3.25
d	16	h	1.6

## 2.2. Antenna Design Evolution Stages

A six-stage step-by-step design evolution procedure for the antenna is illustrated in Fig. 3. Antenna I has a square slot cut in the ground. The dimensions are calculated as a simple patch antenna that resonates around 3.5 GHz. Subsequently, diagonal tabs are added to the slot to facilitate circular polarization, thereby loading the patches approximately with the dimensions of 5 GHz makes resonance at a second frequency band. Antenna III has two plus-shaped slots added to the loaded patches to ease the circular polarization in the higher frequency band; further, they are positioned to tune the axial ratio to the desired frequency of interest. An L-shaped slot is added beneath the microstrip line to increase the bandwidth, as shown in Fig. 4. Later in Antenna V, the H-shaped stub roughly quarter wavelength w.r.t the higher frequency is added to tune the axial ratio at the higher frequency band. The diagonal strip helps suppress the lower mode to the H-shaped strip in Antenna VI.

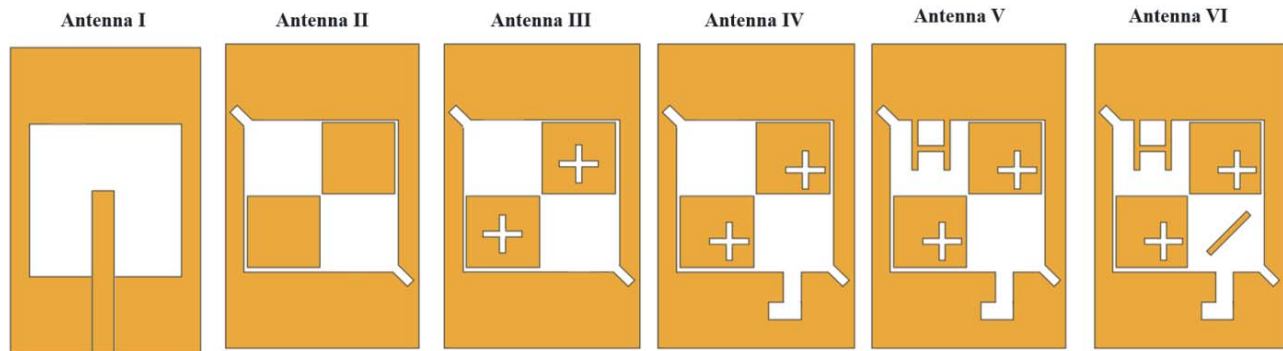


**Figure 3.** Antenna development stages.

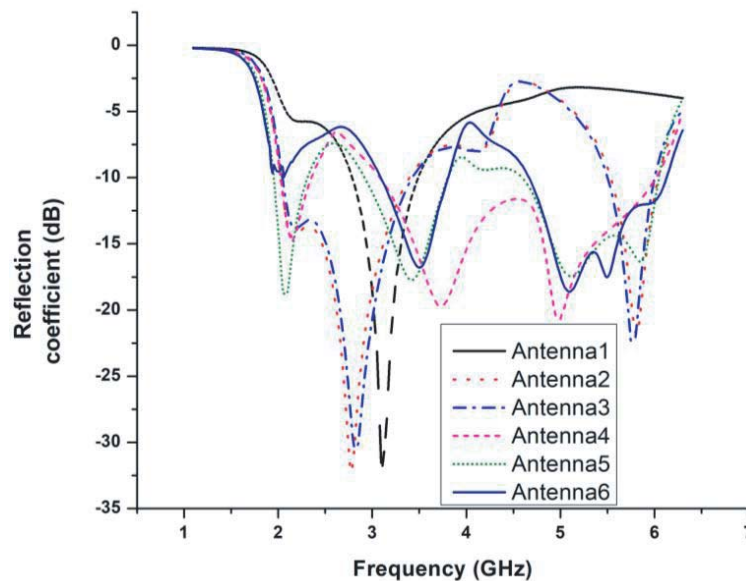
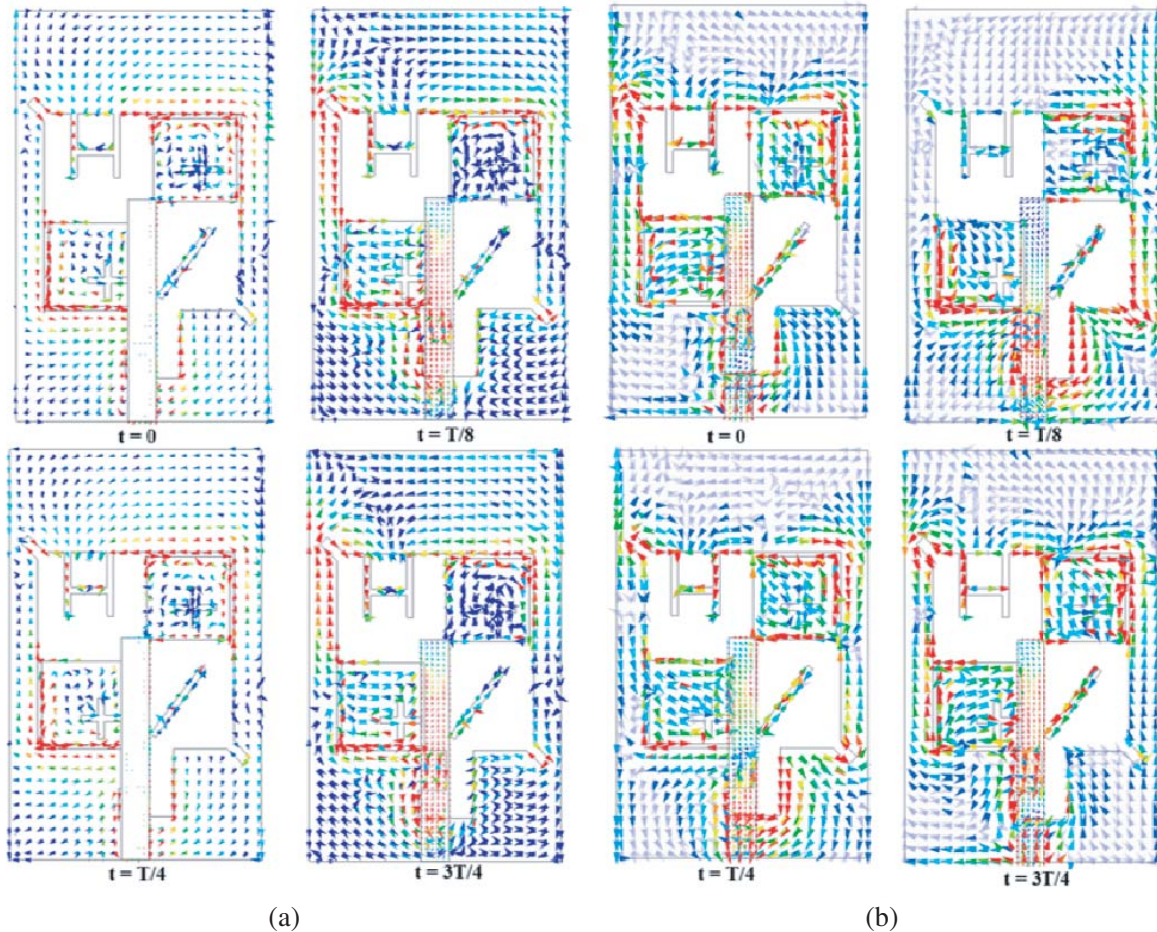


**Figure 4.** Simulated reflection coefficient for antenna I-V.

## 2.3. Parametric Optimization of the Proposed Antenna

A detailed parametric analysis has been carried out with the functional variables of the design. To precisely determine the effect of these parameters on the return loss characteristics, the parameters are varied one at a time, making the others constant. The optimized values of the proposed antenna are shown in Table 1.

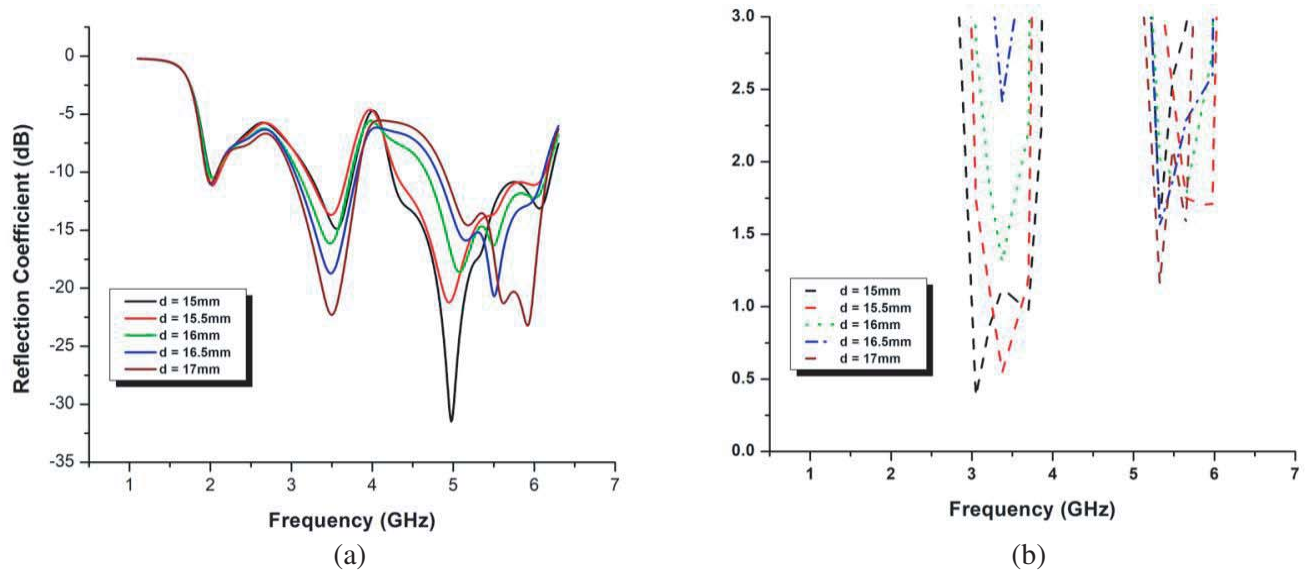
The distribution of surface currents on the rectangular slot antenna operating at 3.5 GHz depicted in Fig. 5 shows that the two parasitic squares loaded at the corners and the L-shaped slot etched in the ground affect the radiation in the lower frequency. The orientation of the field components is clockwise, and as the maximum radiation is aligned outward ( $+z$ -axis), it is Left Hand Circularly Polarized (LHCP). The parametric analysis has been carried out in Ansys HFSS [19], shown in Figs. 6–8. The rectangular microstrip slot antenna radiates in the left-hand circular polarization sense in the direction of maximum radiation for 3.5 GHz and 5.5 GHz. The proposed antenna can be converted into an Right Hand Circularly Polarized (RHCP) dominant polarization by mirroring the slot cut in the ground plane.



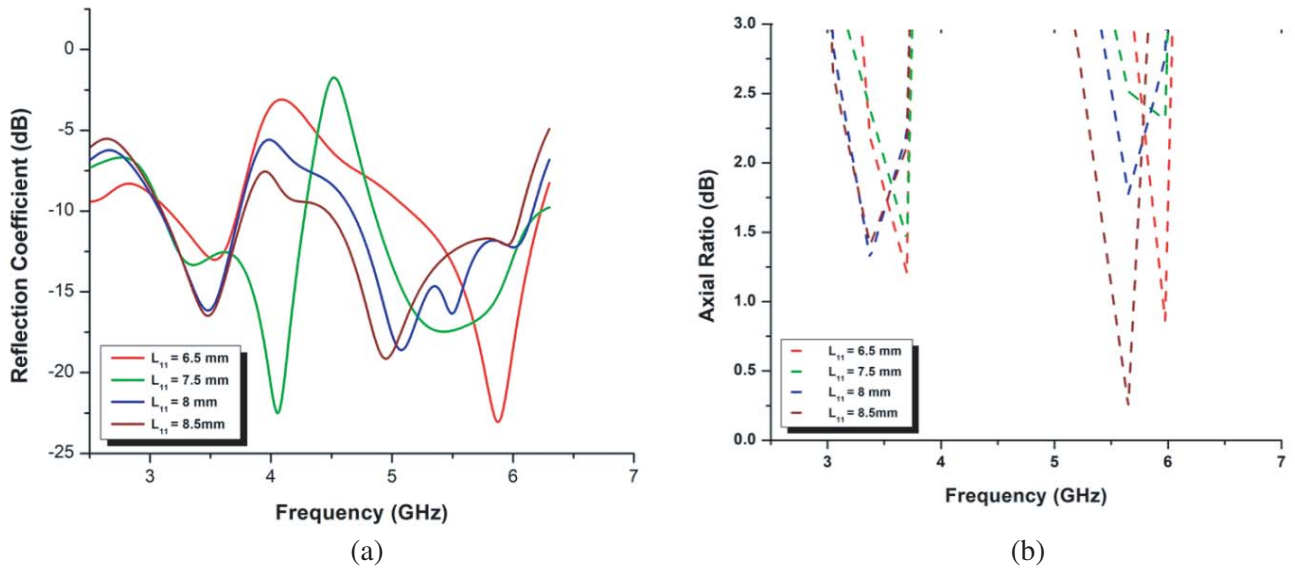
**Figure 5.** Surface currents at (a) lower band 3.5 GHz (b) upper band 5.5 GHz.

Figure 6 depicts the effects of varying distance ' $d$ ' on  $S_{11}$  and axial ratio bandwidth. As the value ascends from 15 mm to 17 mm, the reflection coefficient graph in the lower frequency band is tuned much better. On the other hand, we can see the higher frequency band upshifting and having a balance maintained in tuning both the lower and upper-frequency bands in the desired range. The main emphasis is on achieving a broader axial ratio bandwidth value of 16 mm which is chosen as it satisfies a wider bandwidth condition for both the impedance and axial ratio bandwidths.

Figure 7 illustrates the impact of varying the length  $L_{11}$  on the reflection coefficient and axial ratio plots as the value ranges from 6.5 mm to 8.5 mm. As  $L_{11}$  descends, a significant effect is found on the lower- and upper-frequency bands. The lower frequency starts deteriorating, and the upper-frequency band tends to upshift, showing transference from the desired range. Hence, a nominal value of 8 mm is chosen to maintain both the frequency bands evened concerning impedance and axial ratio bandwidths.



**Figure 6.** Effect of  $d$  on (a) reflection coefficient and (b) axial ratio.



**Figure 7.** Effect of length  $L_{11}$  on (a) reflection coefficient and (b) axial ratio.

The effect of varying length  $W_{11}$  on  $S_{11}$  and the axial ratio plots are illustrated in Fig. 8. As the value varies from 3 mm to 4 mm, there is a significant change in the reflection coefficient at  $W_{11} = 3.5$  mm; we can see that the impedance curve is matched comparatively better. The axial ratio plot shows a good polarization purity, and a broader bandwidth has been achieved. Above all, the parasitic square shapes, H shape, and the loaded slant strip contribute by providing enhanced bandwidth and the required rotation aiding the polarization ability.

### 3. RESULTS

A rectangle-shaped slot antenna loaded with parasitic squares is simulated and designed on a low-cost dielectric substrate (FR-4), with dielectric constant ( $\gamma_r$ ) = 4.4 and operating frequencies of 3.5 GHz and 5.32 GHz. The design parameters are listed in Table 1. The structure and design model are shown in

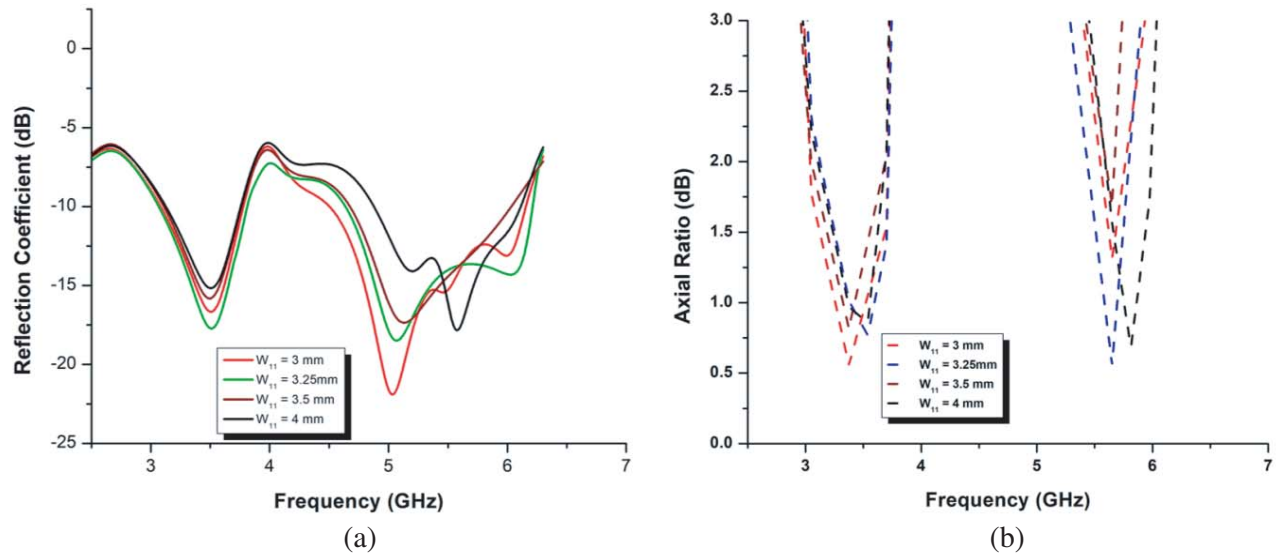


Figure 8. Effect of length  $W_{11}$  on (a) reflection coefficient and (b) axial ratio.

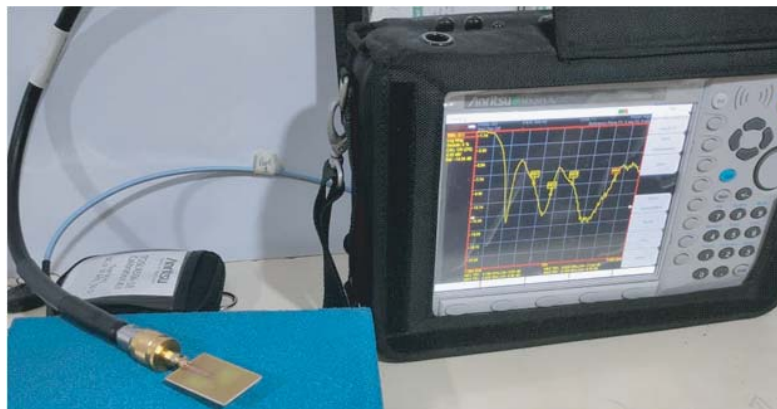
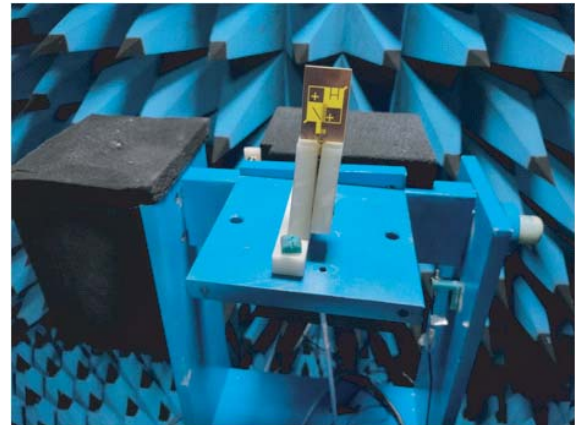
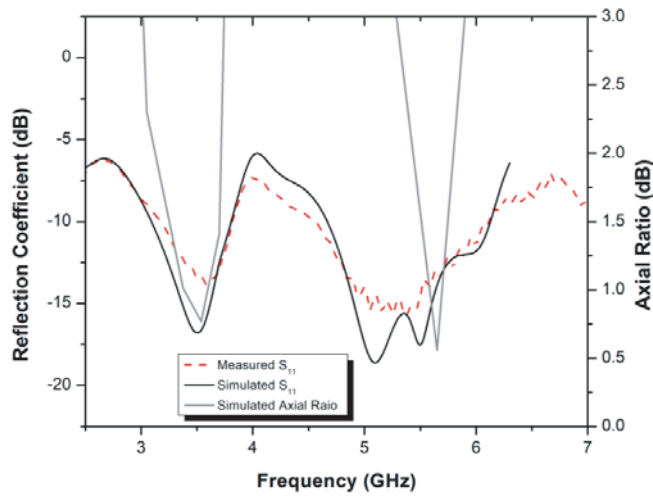


Figure 9. Network analyzer measurement setup.

Fig. 1. The finite element method-based solver High-Frequency Structure Simulator (HFSS) is used for the microstrip antenna modeling and simulation. The measurement setup for the reflection coefficient taken in Anritsu Network Analyzer (MS2037C) is presented in Fig. 9.

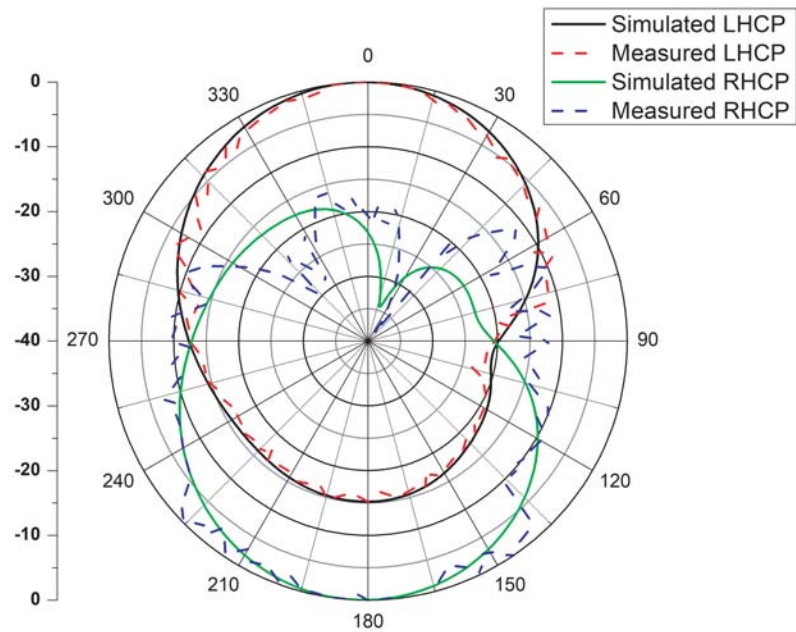
The simulated and experimental reflection coefficients ( $S_{11}$  in dB) of the designed slot antenna are shown in Fig. 10. The simulated results depict that the reflection coefficients are  $\leq -10$  dB at 3.5 GHz and 5.5 GHz, respectively. The experimental reflection coefficient for the frequency range  $\leq -10$  dB plots match the simulated results in the desired bandwidth range of 640 MHz (3.06 GHz to 3.73 GHz) for the lower frequency band and 1.57 GHz (4.64 GHz to 6.21 GHz) for the upper-frequency band. From Fig. 10, it is clear that the axial ratio bandwidth overlaps with the impedance bandwidth range, i.e., with a usable C.P. bandwidth of 90% in the lower frequency band and 37.5% in the upper-frequency band. The simulated axial ratio bandwidths for the lower frequency band and upper-frequency band are 670 MHz and 590 MHz.

Figure 11 depicts an anechoic chamber setup used in measuring the radiation patterns for the rectangle-shaped slot-based microstrip antenna. The far-field normalized radiation patterns of the proposed antenna at the lower- and upper-frequency bands are depicted in Fig. 12 and Fig. 13. The far-field patterns describe that the antenna radiates in LHCP in the upper hemisphere for both the lower- and upper-frequency bands. Fig. 12 presents the comparison plots between the simulated and



**Figure 10.** The simulated and measured antenna reflection coefficients and axial ratio.

**Figure 11.** Measurement setup in anechoic chamber.



**Figure 12.** Measured and simulated radiation patterns at 3.5 GHz.

measured radiation patterns of the antenna for 3.5 GHz and shows a reasonable agreement with the simulated and measured radiation patterns. The antenna gain obtained is 3.2 dB, and it is LHCP.

Figure 13 depicts the simulated and measured radiation patterns of the rectangle-shaped slot-based microstrip antenna for 5.5 GHz. The antenna gain obtained is 1.6 dB, and it is LHCP polarized. Table 2 provides a performance comparison with a few existing works in the literature.

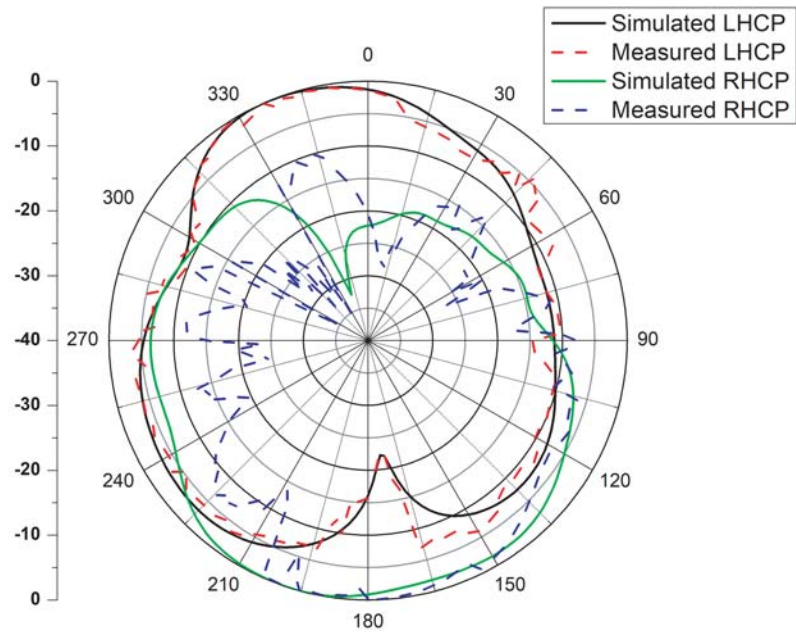


**Figure 13.** Measured and simulated radiation patterns at 5.5 GHz.

**Table 2.** Comparison of existing works of literature with the proposed work.

Reference	Resonant Frequency/Band (GHz)	Size (mm <sup>3</sup> )	Impedance Bandwidth (%)	Axial Ratio Bandwidth (MHz)	Polarization
[20]	2.73	54 × 54 × 0.8	81.6	2060	LHCP
[21]	0.9, 2.45	150 × 150 × 9.2	5,10, 4	-	RHCP
[22]	4.75	60 × 60 × 1.6	12.5	55	RHCP and LHCP simultaneous for transmission and reception
[23]	1.83, 2.5, 3.1	50 × 50 × 1.6	21.4, 12.8, 4.5	8, 30, 11	LHCP
Proposed Work	3.5, 5.5	48 × 29.5 × 1.6	21.5, 29.4	670, 590	LHCP

#### 4. CONCLUSION

A simple broadband rectangle-shaped slot antenna loaded with parasitic square shapes for dual-band circular polarization is presented. The L-shaped stub added beneath the microstrip feed line and the wide slot ensure the polarization purity and enhanced bandwidth. The axial ratio bandwidth overlaps with the impedance bandwidth range, i.e., with a usable C.P. bandwidth of 90% in the lower-frequency band and 37.5% in upper-frequency band. The proposed antenna is best suited for 3.5/5.5 GHz WiMAX band applications.

## ACKNOWLEDGMENT

The authors would like to thank Dr. Jagdish Kumar M Rathod, Associate Dean (&) Professor BVM Engineering College, Anand, Gujarat, for his extended support in providing the testing facilities.

## REFERENCES

1. James, J. R., P. S. Hall, and C. Wood, *Microstrip Antenna*, Peter Peregrinus, 1981.
2. Haneishi, M. and S. YYoshida, "A design method of circularly polarised rectangular microstrip antenna by one-point feed," *Electronics and Communication*, Japan, 1981.
3. Zhao, J.-Y., Z.-Y. Zhang, Y. Li, G. Fu, and S.-X. Gong, "Wideband patch antenna with stable high gain and low cross-polarization characteristics," *Progress In Electromagnetics Research Letters*, Vol. 45, 35–38, 2014.
4. Lam, K. Y., K.-M. Luk, K. F. Lee, H. Wong, and K. B. Ng, "Small circularly polarized U-slot wideband patch antenna," *IEEE Antennas and Wireless Propagation Letters*, Vol. 10, 87–90, 2011.
5. Haneishi, M., T. Nambara, and S. Yohsida, "Study on elliptical properties of singly-fed circularly polarised microstrip antennas," *Electronics Letters*, Vol. 18, 191–193, 1982.
6. Chen, W.-L., G.-M. Wang, and C.-X. Zhang, "Bandwidth enhancement of a microstrip-line-fed printed wide-slot antenna with a fractal-shaped slot," *IEEE Transactions on Antennas and Propagation*, Vol. 57, No. 7, 2176–2179, 2009.
7. Rahimi, M., M. Maleki, M. Soltani, A. S. Arezomand, and F. B. Zarrabi, "Wide band SRR-inspired slot antenna with circular polarization for wireless application," *AEU — International Journal of Electronics and Communications*, Vol. 70, No. 9, 1199–1204, 2016.
8. Cao, R. and S.-C. Yu, "Wideband compact CPW-fed circularly polarized antenna for universal UHF RFID reader," *IEEE Transactions on Antennas and Propagation*, Vol. 63, No. 9, 4148–4151, 2015.
9. Yang, F. and Y. Rahmat-Samii, "Switchable dual-band circularly polarised patch antenna with single feed," *Electronics Letters*, Vol. 37, No. 16, 1002, 2001.
10. Beigmohammadi, G., C. Ghobadi, J. Nourinia, and M. Ojaroudi, "Small square slot antenna with circular polarisation characteristics for WLAN/WiMAX applications," *Electronics Letters*, Vol. 46, No. 10, 672–673, 2010.
11. Ojaroudi, M., C. Ghobadi, and J. Nourinia, "Small square monopole antenna with inverted t-shaped notch in the ground plane for uwb application," *IEEE Antennas and Wireless Propagation Letters*, Vol. 8, 728–731, 2009.
12. Ellis, M. S., Z. Zhao, J. Wu, X. Ding, Z. Nie, and Q. Liu, "A novel simple and compact microstrip-fed circularly polarized wide slot antenna with wide axial ratio bandwidth for C-band applications," *IEEE Transactions on Antennas and Propagation*, Vol. 64, No. 4, 1552–1555, 2016.
13. Wang, L., Y. X. Guo, and W. X. Sheng, "Tri-band circularly polarized annular slot antenna for GPS and CNSS applications," *Journal of Electromagnetic Waves and Applications*, Vol. 26, Nos. 14–15, 1820–1827, 2012.
14. Xu, R., J. Li, Y. Qi, G. W. Yang, and J. Yang, "A design of triple-wideband triple-sense circularly polarized square slot antenna," *IEEE Antennas and Wireless Propagation Letters*, Vol. 16, 1763–1766, 2017.
15. Niyamanon, S., R. Senathong, and C. Phongcharoenpanich, "Dual-frequency circularly polarized truncated square aperture patch antenna with slant strip and L-shaped slot for WLAN applications," *International Journal of Antennas and Propagation*, 11, 2018.
16. Deng, I.-C., J.-B. Chen, Q.-X. Ke, J.-R. Chang, W.-F. Chang, and Y. King, "A circular CPW-fed slot antenna for broadband circularly polarized radiation," *Microwave Optical Technology Letters*, Vol. 49, 2728–2733, 2007.
17. Chandu, D. S. and S. S. Karthikeyan, "A novel broadband dual circularly polarized microstrip-fed monopole antenna," *IEEE Transactions on Antennas and Propagation*, Vol. 65, No. 3, 1410–1415, 2017.

18. Altaf, A., Y. Yang, K.-Y. Lee, and K. C. Hwang, "Wideband circularly polarized Spidron fractal slot antenna with an embedded patch," *International Journal of Antennas and Propagation*, 2017.
19. *Ansys HFSS version 2020 R1*.
20. Trinh-Van, S., Y. Yang, K.-Y. Lee, and K. C. Hwang, "Broadband circularly polarized slot antenna loaded by a multiple-circular-sector patch," *Sensors*, Vol. 18, 1576, 2018.
21. Phongcharoenpanich, K. B. C. and S. Kosulvit, "Dual-band circular plate antenna with annular-ring slot and four-paired rectangular slots," *2013 10th International Conference on Electrical Engineering/Electronics, Computer, Telecommunications and Information Technology IEEE*, 1–4, 2013.
22. Bharath Reddy, G., M. Harish Adhithya, and D. Sriram Kumar, "Simultaneously RHCP and LHCP radiating polarization diversity C-slot antenna for mobile satellite communications," *IETE Journal of Research*, 2019.
23. Paul, P. M., K. Kandasamy, and M. S. Sharawi, "A triband circularly polarized strip and SRR-loaded slot antenna," *IEEE Transactions on Antennas and Propagation*, Vol. 66, No. 10, 5569–5573, 2018.